JOURNAL OF THERMOPHYSICS AND HEAT TRANSFER
Vol. 18, No. 4, October–December 2004

Elemental Demixing in Air and Carbon Dioxide Stagnation Line Flows

P. Rini* and G. Degrez†
von Kármán Institute for Fluid Dynamics, 1640 Rhode-St.-Genèse, Belgium
and
Université Libre de Bruxelles, 1050 Bruxelles, Belgium

The influence of elemental fraction variations on the computation of thermochemical equilibrium flows is analyzed for both air and carbon dioxide mixtures. First the thermochemical equilibrium stagnation line equations for a mixture of perfect gases are presented for both the cases of constant and variable elemental fractions. Then, the equilibrium computations are compared with several chemical regimes to better analyze the influence of chemistry on wall heat flux and to observe the elemental fractions behavior along a stagnation line. The results of several computations are presented to highlight the effects of elemental demixing on the stagnation point heat flux and chemical equilibrium composition for air and carbon dioxide mixtures. Moreover, in the chemical nonequilibrium computations, the characteristic time of chemistry is artificially decreased and in the limit the chemical equilibrium regime, with variable elemental fractions, is achieved. Finally the effects of outer edge elemental fractions on the heat flux map is analyzed, showing the need to add them to the list of parameters of the methodology currently used to determine catalycity properties of thermal protection materials.

Nomenclature

c_i = concentration of species i
F = streamfunction
g = mixture nondimensional enthalpy
h = mixture enthalpy
h_i = enthalpy of species i
$\boldsymbol{J}_i$ = diffusion flux of species i
$\tilde{\mathcal{J}}_i$ = nondimensional diffusion flux of species i
K_c = equilibrium constant
k_b = backward reaction rate
k_f = forward reaction rate
M_i = molar mass of species i
N_{el} = number of elements
N_r = number of reactions
N_{sp} = number of species
Pr = Prandtl number
r = local radius of the probe
T = mixture temperature
u = component of the velocity in the x direction
$\tilde{V}$ = nondimensional velocity in the $\hat{\eta}$ direction
$\dot{\mathcal{W}}_i$ = nondimensional mass production term of species i
y = physical coordinate normal to the body
y_i = mass fraction of species i
X_i = any chemical species
x = physical coordinate along the body contour
x_{ni} = elemental fraction of element i
$\hat{\eta}$ = second Lees–Dorodnitsyn coordinate
μ = dynamic viscosity
ν'_{ir} = stoichiometric coefficient of species i thought as reactant in reaction r
ν''_{ir} = stoichiometric coefficient of species i thought as product in reaction r
ξ_j = number of moles of element j per unit volume
$\xi(x)$ = first Lees–Dorodnitsyn coordinate
ρ = mixture density
ρ_i = partial density of species i
ϕ_i^c = number of elements of type c in the species i
$\dot{\omega}_i$ = mass production due to chemical reactions

Subscripts

δ = boundary-layer edge
w = wall

Introduction

THE von Kármán Institute is actively involved in the determination of catalytic properties of thermal protection system (TPS) materials. A hybrid methodology, which relies on the combination of experimental measurements and numerical calculations, has been employed for this purpose. The principles of this methodology lay on the local heat transfer simulation (LHTS) concept developed at the Institute for Problems in Mechanics of Moscow (IPM).[1]

A critical output of the LHTS methodology is the heat load on the stagnation point of a flying body, where large gradients in temperature and mass concentrations are present. These features make this point a suitable benchmark for testing thermochemical models. Among all of the assumptions on which the previous methodology are based, this paper is especially focused on the analysis of the effects of the elemental fractions variation, that is, the elemental demixing effect. Indeed, in the original Russian methodology developed at IPM, both the local thermal equilibrium (LTE) simulations of an inductively coupled plasma (ICP) facility[2–4] and the chemical nonequilibrium stagnation line flow computations, needed to determine the catalytic activity of TPS materials, are carried out assuming constant elemental fractions. A theoretical description of elemental demixing in LTE conditions is proposed in Ref. 5, where a general formulation of the equations for a multicomponent mixtures in thermochemical equilibrium is presented. Moreover a previous attempt to investigate diffusion separation of chemical elements on a catalytic surface was proposed by Kovalev and Suslor in Ref. 6. There, for a large Schmidt number, an asymptotic expansion of the solution, of the boundary-layer equations for a multicomponent air mixture in chemical nonequilibrium is used. It is shown that an excess of a mixture element can be observed on the body under certain

Received 5 December 2003; revision received 6 February 2004; accepted for publication 6 February 2004.

*Ph.D. Candidate, Department of Aeronautics and Aerospace, 72, Ch. de Waterloo; also Assistant, Service de Mécanique des Fluides, 50, Avenue F. D. Roosevelt; rini@vki.ac.be. Member AIAA.

†Adjunct Professor, Department of Aeronautics and Aerospace, 72, Ch. de Waterloo; also Professor, Service de Mécanique des Fluides, 50, Avenue F. D. Roosevelt; degrez@vki.ac.be. Associate Fellow AIAA.

outer edge conditions. Although pioneering, the study was based on some simplifications, such as a large Schmidt number and constant ratio $\rho\mu/(\rho_w\mu_w)$, which are removed in the present computations. Indeed, no hypothesis is made on the magnitude of Schmidt number, and both density and viscosity are computed independently, making the present approach more general than the one proposed in Ref. 6.

To investigate the validity of the constant elemental fraction assumption, attention is focused on the simulation of the stagnation line flow, where the influence of demixing on chemical equilibrium computations is analyzed. In the next section, a preliminary analysis of the influence of elemental fractions on the chemical composition is presented. Then follows the presentation of the equations solved to analyze a thermochemical equilibrium stagnation line flow for the two conditions of constant and variable elemental fractions. From an analytical point of view, the difference between these two cases of interest is in the way the chemical composition is computed. Indeed, when thermochemical equilibrium is assumed, the mixture composition depends on the local values of temperature, pressure, and elemental fractions. If the presence of demixing is neglected, the elemental fractions remain constant and equal to the outer edge values. On the other hand, if one allows for elemental demixing, the elemental fractions become additional unknowns, and suitable conservation equations must be solved to compute correctly the elemental composition.

Influence of Elemental Fractions on Thermochemical Equilibrium Composition

It is well known that the composition of a mixture of reacting gases under thermochemical equilibrium can be expressed as a function of pressure, of temperature, and of the elemental fractions of the elements shared among the mixture species.[7] A preliminary analysis of the influence of the variation of the latter set of parameters on the composition is presented in the following subsections for both air and carbon dioxide mixtures.

Air Mixture

Consider an air mixture composed of the following 11 species: N_2, O_2, NO, N, O, N_2^+, O_2^+, NO^+, N^+, O^+, and e^-. Let us define a reference mixture characterized by elemental fractions $x_{nO} = 0.21$ and $x_{nN} = 0.79$ and two additional mixtures obtained by perturbing the oxygen fraction by an amount of $\pm 10\%$, that is, $x_{nO} = 0.231$, $x_{nN} = 0.769$ and $x_{nO} = 0.189$, $x_{nN} = 0.811$. In Figs. 1–3 the composition of these mixtures are shown as a function of temperature for a fixed pressure of 1 atm, assuming thermochemical equilibrium conditions. From Figs. 1–3, it appears that the species mole fraction is little affected by the elemental fraction, whose influence is basically limited to a scaling of the various species according to the elemental fraction. This is because, in the air mixture, there are only two species including both N and O atoms, that is, NO and NO^+, and in addition, their concentrations always remains small.

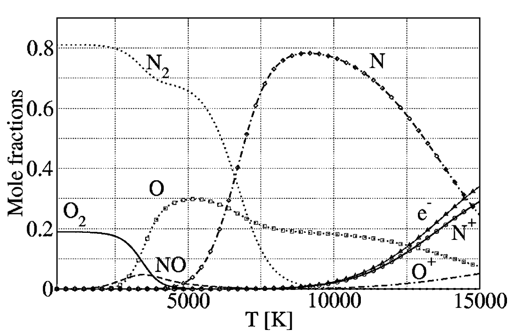

Fig. 1 Mole fractions, $x_{nO} = 0.189$ and $x_{nN} = 0.811$.

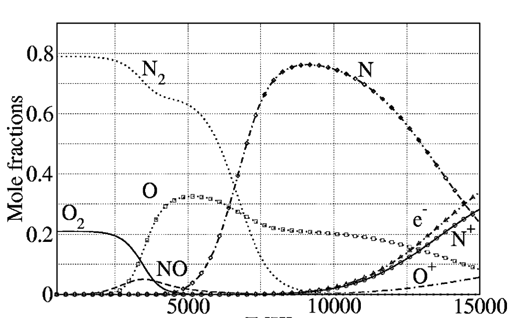

Fig. 2 Mole fractions, $x_{nO} = 0.21$ and $x_{nN} = 0.79$.

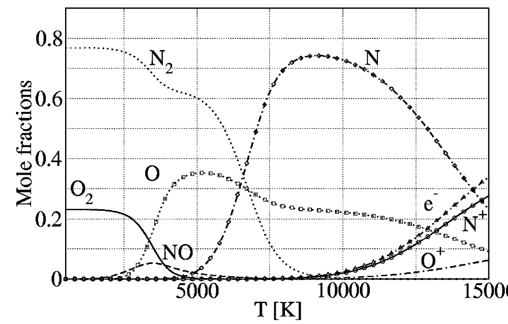

Fig. 3 Mole fractions, $x_{nO} = 0.231$ and $x_{nN} = 0.769$.

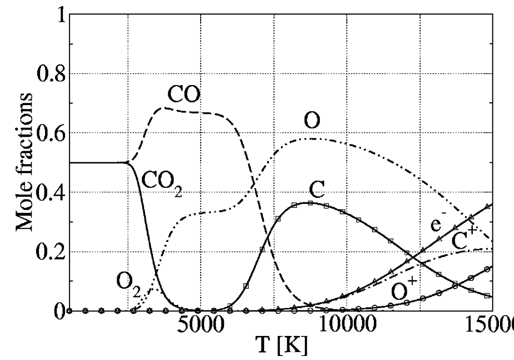

Fig. 4 Mole fractions, $x_{nO} = 18/30$ and $x_{nC} = 12/30$.

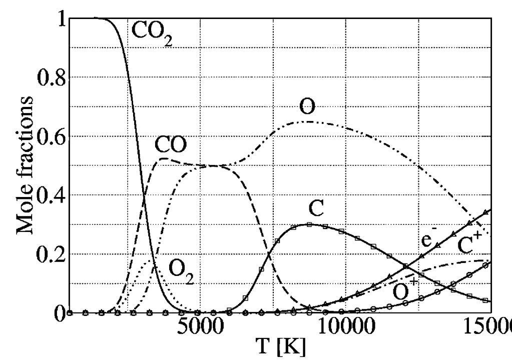

Fig. 5 Mole fractions, $x_{nO} = 2/3$ and $x_{nC} = 1/3$.

CO_2 Mixture

For carbon dioxide mixtures, the sensitivity of the chemical composition to elemental fraction variations is much higher than for air. Indeed, if one considers an eight species mixture[8] in chemical equilibrium composed of CO_2, O_2, CO, C, O, C^+, O^+, and e^- and computes the chemical composition as a function of temperature for a fixed pressure, very different results are obtained depending on the elemental fraction used. Consider a reference mixture characterized by elemental fractions $x_{nO} = 2/3$ and $x_{nC} = 1/3$. Perturbing by $\pm 10\%$ the oxygen fraction, two new mixtures are defined: $x_{nO} = 22/30$, $x_{nC} = 8/30$ and $x_{nO} = 18/30$, $x_{nC} = 12/30$. For a pressure of 1 atm, the mole fraction evolution as a function of temperature is shown in Figs. 4–6 for these three cases. A very strong influence of the elemental fraction on the chemical composition is clearly visible. Moreover, in the case of CO_2 mixtures, from the analysis of the earlier results, it follows that the sensibility to elemental fraction variation is much higher than in the case of air.

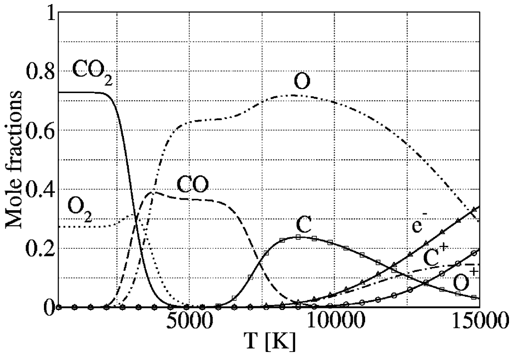

Fig. 6 Mole fractions, $x_{n\mathrm{O}} = 22/30$ and $x_{n\mathrm{C}} = 8/30$.

This will result in an important influence of elemental demixing on heat flux in thermochemical equilibrium CO_2 mixtures, as will be shown.

Thermochemical Equilibrium Stagnation Line Equations

In this section, the governing equations for a chemical equilibrium mixture along a stagnation line are recalled.[8,9] The flow is considered steady, axisymmetric, and laminar; the influence of body forces due to external fields is neglected; and finally, thermochemical equilibrium is supposed.

Among all of the equations describing the current phenomena, the ones related to the determination of the composition represent the only difference between the two cases of presence or absence of demixing. Therefore, first attention is focused on the continuity, momentum, and energy equations, followed by discussion of the two ways in which the composition is computed.

Start from a Cartesian reference system having the x axis lying on the body surface and the y axis normal to it. The Lees–Dorodnitsyn transformation is applied, defining

$$\xi(x) = \int_0^x \rho_\delta \mu_\delta u_\delta r^2 \, \mathrm{d}s \qquad \hat{\eta} = K \frac{u_\delta r}{\sqrt{2\xi}} \int_0^y \rho \, \mathrm{d}t$$

where

$$K = \frac{1}{\delta} \frac{\sqrt{2\xi}}{u_\delta r} \int_0^{\hat{\eta}_{\max}} \frac{1}{\rho} \, \mathrm{d}\hat{\eta}$$

Three new independent variables are introduced as

$$F = \frac{u}{u_\delta}, \qquad g = \frac{h}{h_\delta}, \qquad \tilde{V} = K \frac{2\xi}{\partial \xi / \partial x} \left(F \frac{\partial \eta}{\partial x} + \frac{\rho v r}{\sqrt{2\xi}} \right)$$

where δ is the boundary layer thickness, and r the local radius of the body. Therefore, the stagnation line equations are as follows:

Continuity,

$$\frac{\partial \tilde{V}}{\partial \hat{\eta}} + F = 0 \tag{1}$$

Chemical equilibrium composition is given in the next section.

Momentum,

$$\tilde{V} \frac{\partial F}{\partial \hat{\eta}} = \frac{1}{2} \frac{\rho_\delta}{\rho} \left[1 + \frac{v_\delta}{(\partial u_\delta / \partial x)^2} \frac{\partial}{\partial y} \left(\frac{\partial u_\delta}{\partial x} \right) \right] - \frac{F^2}{2} + \frac{\partial}{\partial \hat{\eta}} \left(\mathcal{K}^2 l_0 \frac{\partial F}{\partial \hat{\eta}} \right) \tag{2}$$

Energy,

$$\tilde{V} \frac{\partial g}{\partial \hat{\eta}} = \frac{\partial}{\partial \hat{\eta}} \left(K^2 \frac{l_0}{Pr} \frac{\partial g}{\partial \hat{\eta}} \right) - \frac{\partial}{\partial \hat{\eta}} \left(K^2 \frac{l_0}{Pr} \sum_{i=1}^{N_{\mathrm{sp}}} \frac{\partial y_i}{\partial \hat{\eta}} \frac{h_i}{h_\delta} \right) - \frac{\partial}{\partial \hat{\eta}} \left(K \sum_{i=1}^{N_{\mathrm{sp}}} \tilde{\mathcal{J}}_i^{\hat{\eta}} \frac{h_i}{h_\delta} \right) \tag{3}$$

The dimensionless diffusion flux $\tilde{\mathcal{J}}_i^{\hat{\eta}}$ is defined as $J_i^y / \sqrt{[2\rho_\delta \mu_\delta (\partial u_\delta / \partial x)]}$. The boundary conditions for the transformed variables are as follows. At the wall $F = 0$ and $g = h_w / h_\delta$, whereas at the outer edge $F = 1$ and $g = 1$. On the other hand, the boundary conditions for the physical variable are at the wall $u = 0$, $v = 0$, and $h = h(T_w)$, whereas at the outer edge $u = u_\delta$, $h = h_\delta$, and $y_i = y_{i,\delta}$.

To solve the differential problem already introduced, one needs to evaluate the thermodynamic, transport, and chemical properties of the mixture. In the von Kármán Institute (VKI) boundary layer code,[9,10] a detailed computation of thermodynamic properties of monoatomic and polyatomic species is performed by means of statistical thermodynamics[11,12] and the diffusion fluxes are obtained solving the Stefan-Maxwell equations (see Refs. 9, 13, and 14).

Chemical Equilibrium Composition

To analyze the influence of demixing in the computation of the composition for a mixture along a stagnation line, two approaches have been followed. First constant elemental fractions, equal to the outer edge values, have been imposed along the stagnation line. Later this constraint has been removed, allowing for elemental fractions to vary, by solving suitable advection diffusion equations. In both cases, a formulation in terms of mole fractions has been used to define the nonlinear system whose solution correspond to the mixture composition for the local temperature, pressure, and elemental fractions.

Constant Elemental Fraction Assumption

Assuming the absence of elemental demixing in the flowfield of interest leads to constant elemental fractions of the elements present in the mixture. For a mixture of N_{sp} species, starting from the number of moles of element c, defined as

$$\xi_c = \sum_{i=1}^{N_{\mathrm{sp}}} \phi_i^c c_i$$

where $c_i = \rho_i / M_i$ and ϕ_i^c is the so-called atomicity coefficient, the elemental fraction of element c reads

$$x_{nc} = \xi_c \bigg/ \sum_{j=1}^{N_{\mathrm{el}}} \xi_j \tag{4}$$

The following equations[11] are solved to compute the chemical composition in terms of mole fractions,

$$\sum_{i=1}^{N_{\mathrm{sp}}} \nu_i^r \overline{x_i} - \ln K_x^r = 0 \qquad r = 1, \ldots, N_r$$

$$\sum_{i=1}^{N_{\mathrm{sp}}} \phi_i^c e^{\overline{x_i}} - \frac{1}{\mathcal{N}/\mathcal{N}_{\mathrm{ref}}} X^c = 0 \qquad c = 1, \ldots, N_{\mathrm{el}}$$

$$\sum_{i=1}^{N_{\mathrm{sp}}} e^{\overline{x_i}} - 1 = 0 \tag{5}$$

where N_r is the number of independent chemical reactions and $\bar{x}_i$ is the natural logarithm of the ith species mole fraction. In the first N_r equations, ν_i^r are the stoichiometric coefficients of the ith species involved in the rth reaction, and K_x^r is the equilibrium constant for the rth reaction. In the last N_{el} equations, X^c is related to the moles of the N_{el} elements by the expression $X^c = \xi_c p / (R_u T)$, where R_u is the universal gas constant and p and T are the gas pressure and temperature.

$\mathcal{N}_{\mathrm{ref}}$ represents the number of moles of a reference mixture, and $\mathcal{N}$ is the number of moles of the mixture at local conditions, which is different from the earlier one because chemical reactions produce changes in the number of moles of a mixture of constant mass. This additional unknown requires an additional equation, which is represented by the constraint that the sum of all mole fractions must be equal to unity.[11]

The mass conservation term X^c has been evaluated as

$$X^c = \sum_{i=1}^{N_{sp}} \phi_i^c x_{i,\mathrm{ref}}$$

where $x_{i,\mathrm{ref}}$ are the mole fractions of the species in a mixture at reference pressure and temperature, which have the same elemental fractions as the outer edge mixture.

Variable Elemental Fraction Assumption

In presence of demixing, the elemental fractions will vary within the boundary layer according to the conservation equations recalled as follows.[8] Consider the species continuity equations for a multicomponent steady gas

$$\mathrm{div}(\rho_i \boldsymbol{u} + \boldsymbol{J}_i) = \dot{\omega}_i \tag{6}$$

where ρ_i is the partial density and $\boldsymbol{J}_i$ the diffusion flux of the ith species. After multiplication by ϕ_i^c and summation among all of the species, Eq. (6) reads

$$\mathrm{div}\left(\underbrace{\sum_{i=1}^{Nsp} \phi_i^c c_i}_{\xi_c} \boldsymbol{u} + \sum_{i=1}^{Nsp} \frac{\phi_i^c \boldsymbol{J}_i}{M_i}\right) = \sum_{i=1}^{Nsp} \phi_i^c \frac{\dot{\omega}_i}{M_i} \tag{7}$$

Because the right term of Eq. (7) is zero, the driving mechanisms for the atoms present in the mixture are explained by

$$\mathrm{div}(\xi_c \boldsymbol{u} + \boldsymbol{N}_c) = 0 \tag{8}$$

where $\boldsymbol{N}_c$ is the number flux of the element c defined as

$$\boldsymbol{N}_c = \sum_{i=1}^{N_{sp}} \phi_i^c \frac{\boldsymbol{J}_i}{M_i} \tag{9}$$

The elemental fraction can, therefore, change along a streamline only thanks to diffusion phenomena. Note that the chemistry has no influence in this balance because it represents only a way in which atoms can be exchanged between various species.

Applying the Lees–Dorodnitsyn transformation, one finally reaches the nondimensional form of the elements conservation equations, which read

$$\frac{\tilde{V}}{\rho}\frac{\partial \xi_c}{\partial \hat{\eta}} - \frac{\tilde{V}}{\rho^2}\frac{\partial \rho}{\partial \hat{\eta}}\xi_c + K\frac{\partial}{\partial \hat{\eta}}\left(\sum_{i=1}^{N_{sp}} \phi_i^c \frac{\tilde{\mathcal{J}}_i^{\hat{\eta}}}{M_i}\right) = 0 \tag{10}$$

Two boundary conditions are required for this equation, at the wall and at the outer edge. In the latter case, the chemical composition is fixed, and from it follows the number of moles per unit volume $\xi_c|_\delta$. On the other hand, at the wall, both the chemical composition and the elemental fractions are unknown; nevertheless, the wall boundary condition can be expressed in terms of the number fluxes of the elements. Indeed, at the wall the value of $\boldsymbol{N}_c$ must be zero for each element, ablation being neglected in the current application. The wall boundary condition has, therefore, been imposed in the form

$$\boldsymbol{N}_c = 0 \qquad c = 1, \ldots, N_{\mathrm{el}} \tag{11}$$

The solution of the elemental conservation equations allows for the determination of the moles of the mixture elements ξ_c and, therefore, of the elemental fractions at any point within the boundary layer. In this way, one does not need to introduce the ratio $\mathcal{N}_{\mathrm{ref}}/\mathcal{N}$ because the term X^c is computed at the actual mixture conditions. Therefore, the solution of the nonlinear system

$$\begin{aligned} &\sum_{i=1}^{N_{sp}} \nu_i^r \overline{x_i} - \ln K_x^r = 0 && r = 1, \ldots, N_r \\ &\sum_{i=1}^{N_{sp}} \phi_i^c e^{\overline{x_i}} - X^c = 0 && c = 1, \ldots, N_{\mathrm{el}} \end{aligned} \tag{12}$$

provides the chemical equilibrium composition of the mixture when demixing is taken into account. As far as the accuracy of the results obtained is concerned, all of the computations presented in the following text are converged for a 100 points discretization of the stagnation line. After a grid convergence study,[8] the chosen number of points were showed to be sufficient to obtain reliable heating predictions.

Air Stagnation Line

An analysis of elemental demixing is done by considering the solution of a stagnation line flow. For Earth entry applications, a five species model composed of N_2, O_2, NO, N, and O has been selected. The flow conditions considered,[15] characteristic of Earth entry, are presented in Table 1. Three different chemical regimes have been analyzed.

First is LTE–no demixing, where the flow is in thermochemical equilibrium and the composition is computed as a function of pressure, temperature, and elemental fractions, and where the latter are supposed to be constant and equal to the outer edge values.

Second is LTE–demixing, where the flow is in thermochemical equilibrium and the composition is computed as a function of pressure, temperature, and elemental fractions, obtained from the solution of Eq. (10).

Third is where the flow is in chemical nonequilibrium (CNEQ) and the composition is computed as the solution of a set of species continuity equations with a fully catalytic wall (FCW) boundary condition. This regime is designated CNEQ–FCW.

In the CNEQ computations, the Dunn–Kang model, as described by Gnoffo et al.,[16] has been used. The wall has been considered to be fully catalytic with respect to oxygen and nitrogen recombination, and the wall reactions chosen are

$$O + (O - s) \rightarrow O_2 \qquad N + (N - s) \rightarrow N_2$$

The wall reaction model of Ref. 17 has been used. The results for an air mixture shown in Fig. 7 are presented in terms of mass fractions,

Table 1 Flow parameters and outer edge conditions

Parameter	Value
T_{wall}	300 K
h_δ	14 MJ/Kg
p_δ	0.1 atm

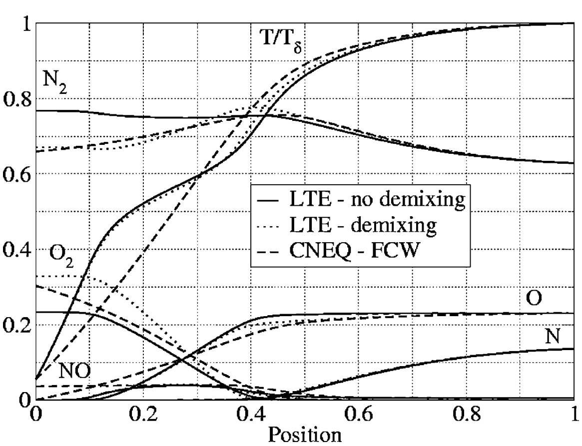

Fig. 7 Mass fraction and nondimensional temperature along the stagnation line [0:w;1:δ].

to analyze the evolution of the chemical composition along the stagnation line. Thanks to the choice of the earlier wall reactions, a fully catalytic surface will promote the formation of O_2 and N_2 molecules. Because the equilibrium composition of a five-species air mixture at the wall temperature of 300 K is characterized mainly by the presence of only O_2 and N_2, one should expect the nonequilibrium fully catalytic wall chemical composition to tend toward the equilibrium one. This happens only if one allows for demixing within the boundary layer, as shown in Fig. 7. Indeed if one neglects the demixing effect, the wall chemical equilibrium composition is far from the nonequilibrium fully catalytic one because of the wrong value of the elemental fractions used in the computation. The analysis of the temperature profiles in Fig. 7 reveals the presence of nonequilibrium phenomena. Indeed the two LTE profiles differ from the CNEQ especially as one approaches the wall, where the gradients are higher for the LTE solutions. On the other hand, the wall species concentrations gradients are higher in the case of CNEQ, the LTE composition being almost constant until a dissociation temperature is reached, in agreement with the results shown at the beginning of the paper. From the earlier considerations, one should expect the conductive part of the heat flux to be higher and the diffusive one to be lower in the LTE cases. These effects on the wall heat flux are mainly balanced, and the values of heat flux for the three chemical regimes are listed in Table 2. Notice that, in the chemical equilibrium case, neglecting the demixing effect leads to a slightly underestimated wall heat flux.

A further investigation of the elemental fraction behavior can be done by considering the elemental balance around the stagnation line. Taking the integral of Eq. (9) over a cylindrical control volume surrounding the stagnation line, one obtains the integral balance[8] for the element c,

$$\xi_{c\delta} V_\delta + N^y_{c\delta} + 2\frac{\partial u_\delta}{\partial x}\left(\delta \Big/ \int_0^{\hat{\eta}_{\max}} \frac{d\hat{\eta}}{\rho}\right)\int_0^{\hat{\eta}_{\max}} \xi_c \frac{F(\hat{\eta})}{\rho}\, d\hat{\eta} = 0 \qquad (13)$$

because the wall element number fluxes are zero.

From Eq. (13) notice that, because the diffusion term is negligible with respect to the other two convective terms, the values of the elemental fraction at the outer edge must be a weighted average of the value of the elements fraction within the boundary layer. Therefore, the difference $x_{nc}(y) - x_{nc}|_\delta$ must be a changing sign nonmonotone function, which physically means that a local excess of elements is compensated by a lack somewhere else along the stagnation line.

In Fig. 8, the behavior of the elemental fraction is shown for different chemical regimes. When absence of demixing is assumed, the elemental fractions remain, of course, constant, and wrong values of the chemical composition are predicted, as shown in Fig. 7. On the other hand the calculations carried out for both the nonequilibrium fully catalytic and the demixing equilibrium cases satisfy the elemental balance. Indeed, for these conditions, Fig. 8 shows the elemental fraction distributions are not in contradiction with Eq. (13).

Table 2 Wall heat flux for three chemical regimes[a]

Chemical regime	q_w, MW/m^2
LTE–demixing	0.660
LTE–no demixing	0.658
CNEQ–FCW	0.656

[a]Here $h_\delta = 14$ MJ/kg and $T_w = 300$ K.

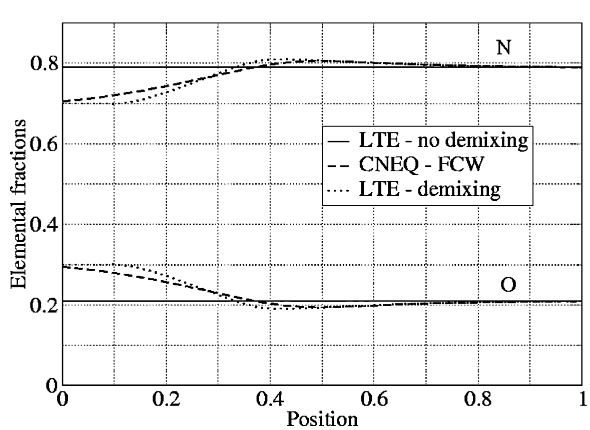

Fig. 8 Elemental fractions along the stagnation line [0:w;1:δ].

Carbon Dioxide Stagnation Line

This section deals with the solution of the stagnation line equations for a CO_2 mixture. The flow parameters considered, characteristic of Mars entry, refer to the test condition of the inductively coupled plasmatron generator (IPG-4) defined in Ref. 18 and are recalled in Table 3. A gas mixture, suitable for Mars entry application, has been considered to be made by five species: CO_2, CO, O_2, C, and O. The same chemical regimes as already discussed have been analyzed. In particular, for the CNEQ computation, the chemical kinetics model of Park et al.[19] has been used, and the wall has been considered fully catalytic with respect to the two following surface reactions:

$$CO + (O - s) \rightarrow CO_2 \qquad O + (O - s) \rightarrow O_2$$

The wall reaction model of Ref. 8 has been used. In Fig. 9, the evolution of the mass fractions along the stagnation line is shown for the three chemical regimes already described. From the analysis of the profiles related to LTE–demixing and no demixing, it appears that significant elemental fraction variations take place in the flow. Indeed, in the case of elemental ratios of $2/3 : 1/3$, 100% CO_2 at the wall is recovered, as expected from the analysis of Fig. 5. However, when elemental demixing is accounted for, the diffusion of carbon elements is responsible for a lower carbon wall fraction than in the case of no demixing, which leads to a lower concentration of CO_2. On the other hand, the oxygen wall fraction increases with respect to the no demixing case, which leads to a nonzero amount of molecular oxygen at the surface.

From the analysis of the CNEQ–FCW results, one notices the presence of nonequilibrium effects that lead to the presence of both CO_2 and O_2 at the surface. As observed for the case of an air mixture, the CNEQ–FCW composition tends toward the equilibrium one only in the case in which elemental demixing is considered. It is of interest to analyze the elements fraction evolution along the stagnation line as in Fig. 10. The elemental fractions variations are clearly observed.

Table 3 Flow parameters and outer edge conditions

Parameter	Value
T_{wall}	300 K
h_δ	15.3 MJ/Kg
p_δ	5.8×10^{-2} atm

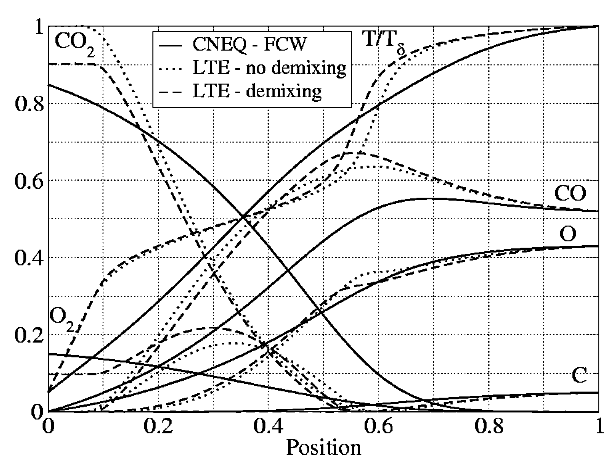

Fig. 9 Mass fraction and nondimensional temperature along the stagnation line [0:w;1:δ].

Table 4 Wall heat flux for three chemical regimes[a]

Chemical regime	q_w, MW/m^2
LTE–no demixing	0.886
LTE–demixing	0.857
CNEQ–FCW	0.856

[a]Here $h_\delta = 15.3$ MJ/kg and $T_w = 300$ K.

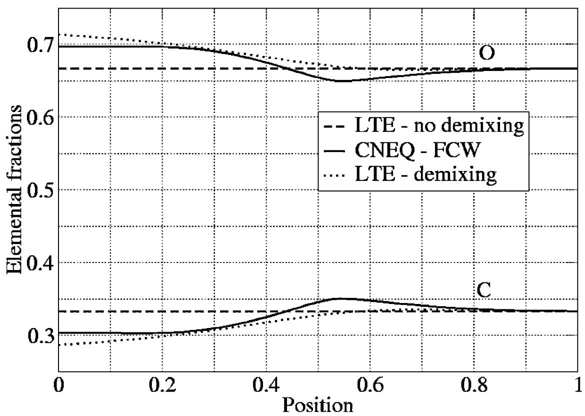

Fig. 10 Elemental fraction along the stagnation line [0:w;1:δ].

Moreover, the elements fractions in the two cases of LTE–demixing and CNEQ–FCW are seen to be very close. Indeed, in both cases the carbon wall fraction decreases and the oxygen fraction increases with respect to the no demixing computation; this leads to a lower carbon dioxide concentration and to a higher O_2 concentration. The decrease of carbon wall fraction from the LTE–no demixing to the CNEQ–FCW condition is followed by the decrease of wall heat flux, as summarized in Table 4.

CNEQ Versus LTE Regime

This section aims to discuss and clarify the relation between the CNEQ and the LTE regimes one. From the analysis of Eq. (6), one can identify at least three chemical regimes, depending on the relative magnitude of the convective–diffusive and chemical–source terms. To simplify the analysis, the expression used to compute the mass production term[7] due to chemical reactions is recalled in Eq. (14) for a set of N_r chemical processes of the type

$$\sum_{i=1}^{N_{\rm sp}} \nu'_{i,r} X_i \underset{k_{b,r}}{\overset{k_{f,r}}{\rightleftharpoons}} \sum_{i=1}^{N_{\rm sp}} \nu''_{i,r} X_i$$

where the backward reaction rates are computed as the ratio between the forward and the equilibrium ones. For this set of reactions, the net rate of change of the ith species concentration is

$$\dot{\omega}_i = \sum_{r=1}^{N_r} \omega_{ir} \tag{14}$$

where

$$\omega_{ir} = M_i(\nu''_{i,r} - \nu'_{i,r})k_{f,r}\left\{\prod_{i=1}^{N_{\rm sp}} c_i^{\nu'_{i,r}} - \frac{1}{K_{c,r}}\prod_{i=1}^{N_{\rm sp}} c_i^{\nu''_{i,r}}\right\}$$

When the characteristic time of the chemical processes, τ_c, is much higher than the flow characteristic time τ_f, the flow is said to be frozen. This coincides with a set of very small, zero in the limit, forward reaction rates. Under these conditions, the right-hand side of Eq. (6) is negligible with respect to the left-hand side, and therefore, in a frozen regime the species concentrations follow the equations $\mathrm{div}(\rho_i \boldsymbol{u} + \boldsymbol{J}_i) = 0$. However, if $\tau_c \ll \tau_f$, local equilibrium conditions are approached. This is equivalent to artificially imposing very high values, infinite in the limit, of the forward reaction rates. As a consequence, the convective–diffusive term in Eq. (6) is negligible with respect to each term of the sum expressed by Eq. (14). Therefore, in the equilibrium regime the species continuity equations tend to the limit $\dot{\omega}_i = 0$, which can be satisfied only by an LTE composition, where $K_{c,r}$ are the equilibrium constants computed from statistical thermodynamics.[7] Indeed, if the condition $\mathrm{div}(\rho_i \boldsymbol{u} + \boldsymbol{J}_i) \ll \omega_{ir}$ is satisfied $\forall r$, then from species mass conservation one has

$$\sum_{i=1}^{N_r} \omega_{ir} - \mathrm{div}(\rho_i \boldsymbol{u} + \boldsymbol{J}_i) \approx \sum_{i=1}^{N_r} \omega_{ir} = 0$$

Moreover the composition satisfying the species equations in the limit of local equilibrium conditions is actually coincident with the solution of the nonlinear system (12), as a function of local pressure, temperature, and elemental fractions. The proof of this statement, in contrast with the observations of Ref. 20, is presented in Figs. 11 and 12 for air and carbon dioxide mixtures.

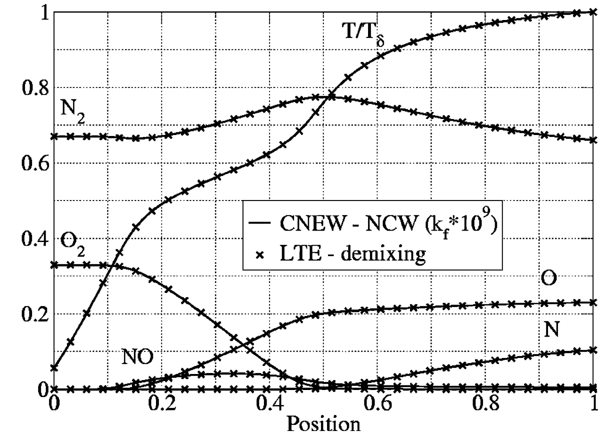

Fig. 11 Air mixture: LTE–demixing vs CNEQ–NCW [0:w;1:δ].

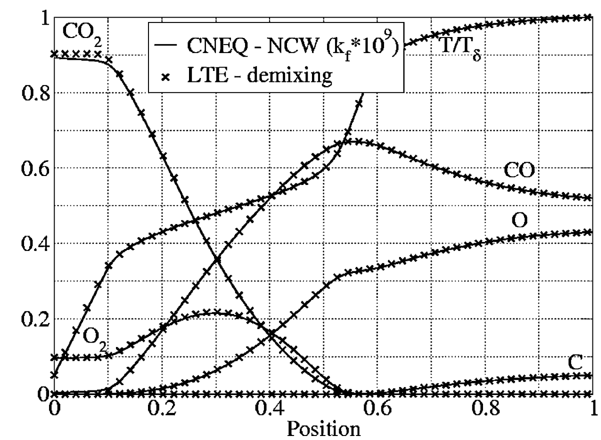

Fig. 12 CO_2 mixture: LTE–demixing vs CNEQ–NCW [0:w;1:δ].

Note that for the CNEQ regime a noncatalytic wall (NCW) has been chosen as the boundary condition for the species continuity equations to let the bulk chemistry drive the species evolution, avoiding any interference with surface reactions. The coincidence of the two computations shows clearly that, if the speed of chemistry is artificially increased, local thermal equilibrium conditions are achieved, provided that the variation of elemental fraction is correctly taken into account by solving elements continuity equations. From a numerical point of view, these results show not only the robustness of the VKI boundary layer code,[9,10] able to solve the stiff problem of infinite rates, but also assess the correctness of the LTE-demixing implementation.

Influence of Outer Edge Elemental Fractions on Heat Flux Maps

As discussed in the Introduction, the methodology developed at the IPM and currently used at VKI to estimate the catalycity properties of TPS materials is based on Navier–Stokes simulations of an ICP facility supposed to be under LTE conditions determined assuming constant elemental fractions. The purpose of the Navier–Stokes plasma flow simulation is to provide the LTE outer edge inputs for the finite thickness nonequilibrium stagnation line flow computations, carried out to compute a heat flux map. Among the quantities needed, the composition is implicitly given as a function of the outer edge pressure and rebuilt enthalpy, assuming LTE and using the torch inlet elemental fractions. In general, thanks to elements diffusion, the elemental fractions vary within the ICP facility[2] leading to an outer edge elemental composition different from the torch inlet one. If this difference has an influence on the heat flux map, by shifting or stretching the isocatalycity lines, the same influence will be reflected in the estimation of TPS material catalycity. One way to estimate easily this influence is to use the results of the constant elemental fraction ICP simulation and to vary only the outer edge elemental fractions, used to determine the outer edge composition for the given enthalpy and pressure.

The results of this analysis are presented in Figs. 13 and 14, which show the heat flux maps corresponding to the discussed conditions for both air and carbon dioxide. The results show an important influence on stagnation point heat flux for carbon dioxide mixtures. The reason for these differences can be explained from the analysis of species concentration shown in Fig. 15 for a fully catalytic cold wall. Indeed, the increase of oxygen outer edge fraction reduces the amount of carbon available for CO_2 recombination at the surface, leading to a lower heat flux. This is more evident for high values of recombination probabilities, where almost the same effect on wall heat flux is observed in the whole temperature range considered. As the recombination probability is reduced, the influence of the outer

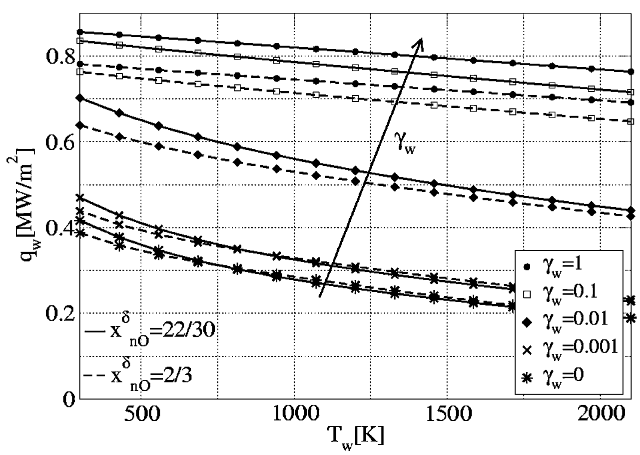

Fig. 13 Influence of outer edge elemental fraction on heat flux map: CO_2 mixture.

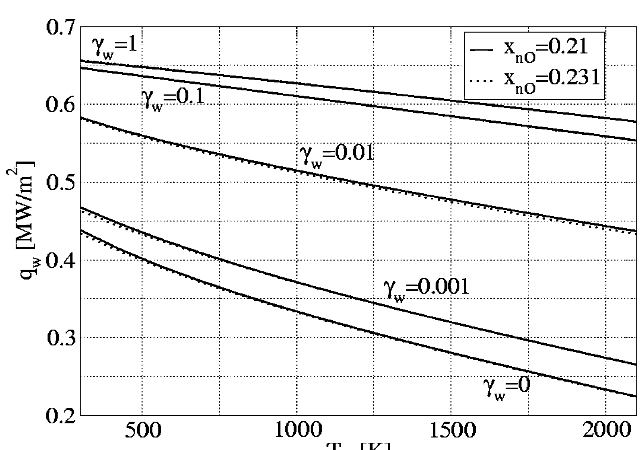

Fig. 14 Influence of outer edge elemental fraction on heat flux map: air mixture.

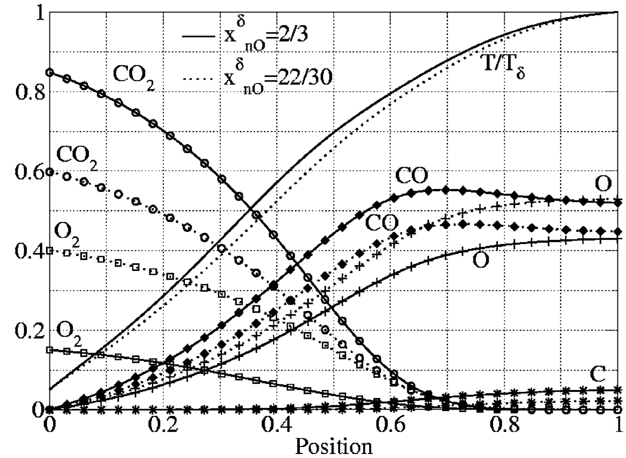

Fig. 15 CO_2 mixture: influence of outer edge elemental fraction on species behavior [0:w;1:δ].

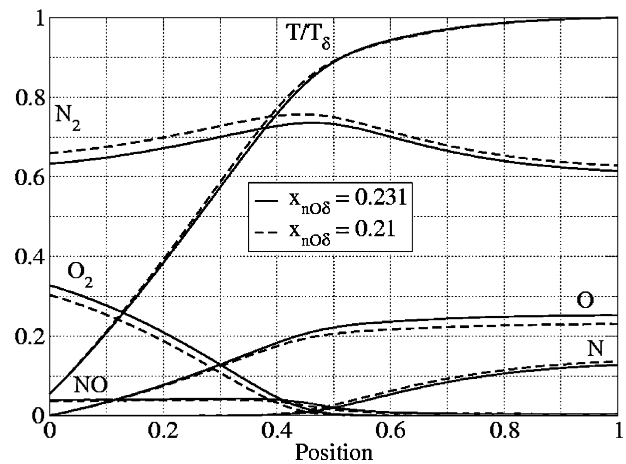

Fig. 16 Air mixture: influence of outer edge elemental fraction on species behavior [0:w;1:δ].

edge elemental fraction decreases as well, and a higher influence is observed for cold wall conditions, where recombination is enhanced by the bulk chemistry because of the low temperature.

For air mixtures, the effects on wall heat flux are essentially negligible. The lines in Fig. 14 are superposed for all values of catalycity in the temperature range investigated. The quite low influence on heat flux can be explained by the analysis of the species mass fraction profiles of Fig. 16. The perturbation of the elements fraction shifts slightly the concentration of N_2, N, and O at the outer edge without altering the stagnation line chemistry very much.

The analysis carried out in this section shows, therefore, that, especially for Mars entry applications, the outer edge elemental fractions play an important role in the determination of the heat flux map and, therefore, in the extrapolation of the TPS material catalycity.

Conclusions

The effects of elemental demixing in thermochemical equilibrium mixtures have been analyzed by means of stagnation line computations. For both air and carbon dioxide flows, nonnegligible elemental fractions variations have been observed, even though for CO_2 mixtures their effects on heat flux are more important. In both cases, the wall composition for a CNEQ regime with FCW is closer to the LTE regime, where the local elemental fraction is computed by solving adequate advection diffusion equations. Moreover, it has been verified that LTE with variable elemental fractions is the limit of a CNEQ regime where the forward reaction rates are artificially increased to sufficiently high values. Finally, the influence of the outer edge elemental fractions on stagnation point heat flux showed the need to add them to the list of parameters of the methodology developed at the IPM, currently used at the VKI to estimate catalycity properties of TPS materials.

References

[1]Kolesnikov, A. F., "Extrapolation from High Enthalpy Tests to Flight Based on the Concept of Local Heat Transfer Simulation," *Measurements Techniques for High Enthalpy and Plasma Flows*, Vol. 8B, von Kármán Inst. Lecture Ser., Rhode-St-Genèse, Belgium, 1999, pp. 1–14.

[2]Vanden Abeele, D., and Degrez, G., "Efficient Computational Model for Inductive Plasma Flows," *AIAA Journal*, Vol. 38, No. 2, 2000, pp. 234–242.

[3]Vasil'evskii, S. A., Kolesnikov, A. F., and Yakushin, M. I., "Mathematical Models for Plasma and Gas Flows in Induction Plasmatrons," *Molecular Physics and Hypersonic Flows*, edited by M. Capitelli, Kluwer, Dordrecht, The Netherlands, 1996, pp. 495–504.

[4]Magin, T., and Degrez, G., "Cooled Pitot Probe in Inductive Air Plasma Jet: What Do We Measure?" 2nd International Symposium Atmospheric Reentry Vehicles and Systems Symposium, Paper 14-83-P, March 2000.

[5]Suslov, O. N., Tirskiy, G. A., and Shchennikov, V. V., "Flows of Multicomponent Ionized Mixtures in Chemical Equilibrium. Description within the Framework of the Navier–Stokes and Prandtl Equations," *Journal of Applied Mechanics and Technical Physics* (in Russian), No. 1, 1971.

[6]Kovalev, V. L., and Suslov, O. N., "Diffusion Separation of Chemical Elements on a Catalytic Surface," *Fluid Dynamics*, Vol. 23, No. 4, 1988, pp. 579–585.

[7]Vincenti, W. G., and Kruger, C. H., *Introduction to Physical Gas Dynamics*, Wiley, New York, 1965.

[8]Rini, P., Garcia, A., Magin, T., and Degrez, G., "Numerical Simulation of CO_2 Stagnation Line Flows with Catalyzed Surface Reactions," *Journal of Thermophysics and Heat Transfer*, Vol. 18, No. 1, 2004, pp. 114–121; also AIAA Paper 2003-4038, June 2003.

[9]Barbante, P. F., "Accurate and Efficient Modeling of High Temperature Nonequilibrium Air Flows," Ph.D. Dissertation, Dept. of Aeronautics and Aerospace, von Kármán Inst., Rhode-Saint-Genèse, Belgium, May 2001.

[10]Barbante, P. F., Degrez, G., and Sarma, G. S. R., "Computation of Nonequilibrium High-Temperature Axisymmetric Boundary-Layer Flows," *Journal of Thermophysics and Heat Transfer*, Vol. 16, No. 4, 2002, pp. 490–497.

[11]Bottin, B., Vanden Abeele, D., Carbonaro, M., Degrez, G., and Sarma, G. S. R., "Thermodynamic and Transport Properties for Inductive Plasma Modeling," *Journal of Thermophysics and Heat Transfer*, Vol. 13, No. 3, 1999, pp. 343–350.

[12]Magin, T., Degrez, G., and Sokolova, I., "Thermodynamic and Transport Properties of Martian Atmosphere for Space Entry Application," AIAA Paper 2002-2226, May 2002.

[13]Magin, T., and Degrez, G., "Transport Properties of Partially Ionized and Unmagnetized Plasmas," *Physical Review E* (to be published).

[14]Magin, T., and Degrez, G., "Transport Algorithms for Partially Ionized and Unmagnetized Plasmas," *Journal of Computational Physics* (to be published).

[15]Garcia, A. M., "Catalycity Effects in Plasmatron Tests," Technical Rept. VKI PR 2001-12, von Kármán Inst. for Fluid Dynamics, Rhode-Saint-Genèse, Belgium, June 2001.

[16]Gnoffo, P. A., Gupta, R. N., and Shinn, J. L., "Conservation Equations and Physical Models for Hypersonic Air Flows in Thermal and Chemical Nonequilibrium," NASA, TP 2867, Feb. 1989.

[17]Scott, D. C., "Catalytic Boundary Conditions in Nonequilibrium Flow," *Proceeding of the IUTAM Symposium Marseille*, edited by R. Brun and A. A. Chikhaoui, Dept. Milleux Hors d'Equilibre, Université de Provence, Marseille, France, 1992, pp. 298–305.

[18]Kolesnikov, A. F., Pershin, I. S., Vasil'evskii, S. A., and Yakushin, M. I., "Study of Quartz Surface Catalycity in Dissociated Carbon Dioxide Subsonic Flows," *Journal of Spacecraft and Rockets*, Vol. 37, No. 5, Sept.–Oct. 2000, pp. 573–579.

[19]Park, C., Howe, J. T., and Jaffe, R. L., "Review of Chemical-Kinetic Problems of Future NASA Missions, II: Mars Entries," *Journal of Thermophysics and Heat Transfer*, Vol. 8, No. 1, 1994, pp. 9–23.

[20]Giordano, D., "The Influence of Medium Compressibility on Chemical Reaction Rates. Part I: Theoretical Considerations," AIAA Paper 2003-4057, June 2003.